Electrical detection of unconventional transverse spin currents in obliquely magnetized thin films

Pieter M. Gunnink [1,*] Rembert A. Duine,[1,2] and Andreas Rückriegel[1]

[1]*Institute for Theoretical Physics and Center for Extreme Matter and Emergent Phenomena, Utrecht University, Leuvenlaan 4, 3584 CE Utrecht, The Netherlands*

[2]*Department of Applied Physics, Eindhoven University of Technology, P.O. Box 513, 5600 MB Eindhoven, The Netherlands*

In a typical experiment in magnonics, thin films are magnetized in plane and spin waves only carry angular momentum along their spatial propagation direction. Motivated by the experiments of Bozhko *et al.* [Phys. Rev. Research **2**, 023324 (2020)], we show theoretically that for obliquely magnetized thin films, exchange-dipolar spin waves are accompanied by a transverse spin current. We propose an experiment to electrically detect this transverse spin current with Pt strips on top of an yttrium iron garnet film, by comparing the induced spin current for spin waves with opposite momenta. We predict the relative difference to be of the order 10^{-4}, for magnetic fields tilted at least $30°$ out of plane. This transverse spin current is the result of the long-range dipole-dipole interaction and the inversion symmetry breaking of the interface.

Introduction. Magnons, or spin waves, are able to transport angular momentum over long distances along their propagation direction [1,2]. This has opened the way to novel signal processing devices which could replace conventional electronic devices [3–5]. In recent years, multiple applications have been explored, such as wave-based computing [6,7], three-terminal transistors [8], logic gates [9,10], and novel nonlinear effects [11,12].

The manipulation of spin waves is still an ongoing area of research and a full toolbox for controlling spin waves is yet to be developed [13]. In this Rapid Communication we consider an alternative approach to control the spin current in a magnetized thin film: by tilting the magnetic field out of plane. This breaks the inversion symmetry and allows a spin current to flow transverse to the propagation direction of the spin waves, transporting angular momentum along the film normal.

This mechanism for generating a transverse spin current was first proposed by Bozhko *et al.* [14], who used a micromagnetic approach to calculate the exchange spin current in a thin film of $Y_3Fe_2(FeO_4)_3$ (YIG), without considering spin absorption at the boundaries. They argued that this spin current is nonzero if the magnetic field is tilted out of plane. However, this transverse spin current can only be detected with an attached spin sink, such as a heavy-metal strip. The interaction with the spin sink significantly influences the physics of the problem. Moreover, only the transfer of angular momentum by the exchange interaction was considered. The dipole-dipole interaction is also capable of transporting angular momentum and therefore needs to be taken into account for a complete description of this system.

In this Rapid Communication we propose an experiment where the transverse spin current in an obliquely magnetized thin film is detected electrically. We consider, within linear spin-wave theory, a thin ferromagnetic film with two leads attached, which pick up the transverse spin current induced by left- and right-moving spin waves via the inverse spin-Hall effect (ISHE) [15]. A transverse spin current would transport more angular momentum into the right spin sink than into the left spin sink, or vice versa. This is equivalent to the experimentally harder to realize system with leads attached to the top and bottom. We propose to compare the spin current picked up by the left and right lead, in order to exclude any usual spin pumping effects, which are also present for an in-plane magnetic field [16]. In order to further understand the origin of the transverse spin current, we show in the Supplemental Material [17] with a magnetostatic calculation that the symmetry breaking at the interface is carried by the dipole-dipole interaction.

Method. The setup we consider is a thin film of ferromagnetic YIG, where coherent spin waves are excited using a coplanar waveguide [18], as depicted in Fig. 1. The wave vector (k) of the excited magnons is controlled by the grating of the antenna and the frequency (ω) of the excited magnons by the frequency of the driving field. To the right and left of this antenna two platinum (Pt) leads are placed which function as spin sinks via the inverse spin-Hall effect and pick up the transverse spin current induced by the spin waves with opposite momenta. The distance between the Pt leads and the coplanar waveguide is assumed to be such that the signal is strong enough to measure small variations. Structures with a separation distance of 3 mm are possible [19], but the magnon diffusion length of $\lambda = 9.4$ μm in YIG [1] indicates that shorter distances would be preferable.

The spin dynamics are governed by the semiclassical Landau-Lifshitz-Gilbert (LLG) equation

$$\partial_t \mathbf{S}_i = \mathbf{S}_i \times \left(-\frac{\partial \mathcal{H}}{\partial \mathbf{S}_i} + \mathbf{h}_i(t) - \frac{\alpha_i}{S} \partial_t \mathbf{S}_i \right), \quad (1)$$
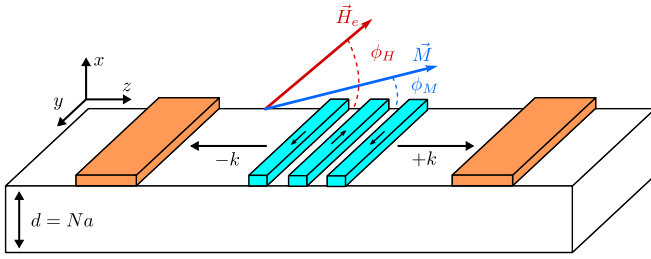
*p.m.gunnink@uu.nl

FIG. 1. The setup considered, with a coplanar waveguide in the middle, exciting spin waves in two opposite directions in a thin ferromagnetic film with thickness d. Two heavy-metal leads pick up the spin current induced by these left- and right-moving spin waves. The magnetic field is tilted out of plane at an angle ϕ_H with the plane and the magnetization has angle ϕ_M with the plane.

where we describe YIG as a Heisenberg ferromagnet with effective spin S, on a cubic lattice. Including both the exchange and dipole-dipole interactions our effective Hamiltonian [20] is

$$\mathcal{H} = -\frac{1}{2} \sum_{ij} J_{ij} \mathbf{S}_i \cdot \mathbf{S}_j - \mu \mathbf{H}_e \cdot \sum_i \mathbf{S}_i$$
$$- \frac{1}{2} \sum_{ij, i \neq j} \frac{\mu^2}{|\mathbf{R}_{ij}|^3} [3(\mathbf{S}_i \cdot \hat{\mathbf{R}}_{ij})(\mathbf{S}_j \cdot \hat{\mathbf{R}}_{ij}) - \mathbf{S}_i \cdot \mathbf{S}_j], \quad (2)$$

where the sums are over the lattice sites $\mathbf{R}_i$, with $\mathbf{R}_{ij} = \mathbf{R}_i - \mathbf{R}_j$ and $\hat{\mathbf{R}}_{ij} = \mathbf{R}_{ij}/|\mathbf{R}_{ij}|$. We only consider nearest-neighbor exchange interactions, so $J_{ij} = J$ for nearest neighbors and 0 otherwise. Here, $\mu = 2\mu_B$ is the magnetic moment of the spins, with $\mu_B = e\hbar/(2m_e c)$ the Bohr magneton. $\mathbf{H}_e$ is the external magnetic field, which we take strong enough to fully saturate the ferromagnet.

To the top of the thin film we attach a spin sink to detect the spin waves, which introduces an interfacial Gilbert damping α_i^L, which is only nonzero for sites at the top interface of the ferromagnet [16]. The total Gilbert damping is then $\alpha_i = \alpha^B + \alpha_i^L$, where α^B is the bulk Gilbert damping. Furthermore, $\mathbf{h}_i(t)$ is the circularly polarized driving field, which we take to be uniform throughout the film. Within linear spin-wave theory, the LLG has been shown to be fully equivalent to the nonequilibrium Green's function formalism [21].

We consider a thin film, infinitely long in the y, z directions and with a thickness $d = Na$ in the x direction, where a is the lattice constant and N is the number of layers. The magnetic field is tilted at an angle ϕ_H with respect to the film, as shown in Fig. 1. The magnetization is tilted by an angle ϕ_M, as determined by minimizing the energy given by Eq. (2) for a classical, uniform spin configuration,

$$\frac{\partial}{\partial \phi_M} \left[-M_s H_e \cos(\phi_M - \phi_H) - 2\pi M_s^2 \cos^2 \phi_H \right] = 0, \quad (3)$$

where $M_s = \mu S/a^3$ is the saturation magnetization and $H_e = |\mathbf{H}_e|$.

We have two reference frames, one aligned with the thin film as described above and one where the z axis is aligned with the magnetization $\mathbf{M}$. We work in the reference frame of the lattice and rotate the spin operators, such that $\mathbf{S}_i \rightarrow \mathcal{R}_y^{-1}(\phi_M)\bar{\mathbf{S}}_i$, where $\mathcal{R}_y(\phi_M)$ is a rotation around the y axis by

angle ϕ_M and $\bar{\mathbf{S}}_i$ are the rotated spin operators, with the $\bar{S}_i^z$ component pointing along the magnetization $\mathbf{M}$.

We linearize in the deviations from the ground state, $b_i = \frac{1}{2}\sqrt{2S}(\bar{S}_i^x + i\bar{S}_i^y)$ and assume translational invariance in the yz plane. The equation of motion for b_i becomes in frequency space

$$\mathbb{G}_k^{-1}(\omega)\boldsymbol{\psi}_k(\omega) = -\mathbf{h}_k(\omega), \quad (4)$$

where $\mathbf{k} = (k_y, k_z)$ and we have introduced the driving field

$$\mathbf{h}_k(\omega) = [\underbrace{h_k(\omega), \dots, h_k(\omega)}_{N \text{ elements}}, \underbrace{h_{-k}^*(\omega), \dots, h_{-k}^*(\omega)}_{N \text{ elements}}]^T, \quad (5)$$

where $h_k(\omega) = \bar{h}_x + i\bar{h}_y$ is the Fourier transform of the rotated driving field. Furthermore, the magnon state vector is

$$\boldsymbol{\psi}_k(\omega) = [b_k(\omega, x_1), \dots, b_k(\omega, x_N),$$
$$b_{-k}^*(\omega, x_1), \dots, b_{-k}^*(\omega, x_N)]^T, \quad (6)$$

and the inverse Green's function is

$$\mathbb{G}_k^{-1}(\omega) = \sigma_3(1 + i\sigma_3\alpha)\omega - \sigma_3\mathcal{H}_k, \quad (7)$$

where we have introduced $\sigma_3 = \text{diag}(1, \dots, 1, -1, \dots, -1)$, $\alpha = \text{diag}(\alpha_1, \dots, \alpha_N, \alpha_1, \dots, \alpha_N)$, and

$$\mathcal{H}_k = \begin{pmatrix} A_k & B_k \\ B_k^\dagger & A_k \end{pmatrix}, \quad (8)$$

which is the Hamiltonian matrix within linear spin-wave theory, with the amplitude factors $[A_k]_{ij} = A_k(x_i - x_j)$ and $[B_k]_{ij} = B_k(x_i - x_j)$. The dispersion is obtained by diagonalizing the inverse Green's function (4) in the absence of damping and spin pumping. The full expressions for the amplitude factors A_k, B_k and the dispersions for different tilting angles of the magnetic field are given in the Supplemental Material [17].

From the equation of motion, Eq. (4), the total spin current injected into the lead is obtained from the continuity equation for the spin,

$$\partial_t \bar{S}_i^z + \sum_j I_{i \rightarrow j}^{\text{ex}} + \sum_j I_{i \rightarrow j}^{\text{dip-dip}} = I_i^\alpha + I_i^h. \quad (9)$$

The explicit form of the terms is given in the Supplemental Material [17]. We find a source and sink term, providing angular momentum via the driving field (I_i^h) and dissipating angular momentum to the lattice and the lead via the Gilbert damping (I_i^α). There are two ways angular momentum can be transferred through the film. First, there is a spin current transferring angular momentum between adjacent sites ($I_{i \rightarrow j}^{\text{ex}}$), which is driven by the exchange interaction. The dipole-dipole interaction also transports angular momentum ($I_{i \rightarrow j}^{\text{dip-dip}}$), but because the dipole-dipole interaction is nonlocal, angular momentum is transferred from and to all other sites. It is therefore not possible to write this as a local divergence and thus as a current. Also note that the dipole-dipole interaction couples the magnons to the lattice, which means that a nonzero dipole-dipole contribution is accompanied by a transfer of angular momentum from and to the lattice.

The measurable quantity is the angular momentum absorbed by the spin sink in the attached lead, which is

TABLE I. Parameters for YIG used in the numerical calculations in this work. Note that S follows from $S = M_s a^3 / \mu$.

Quantity	Value
N	400
a	12.376 Å [22]
S	14.2
$4\pi M_s$	1750 G [23]
J	1.60 K [24]
α^B	7×10^{-4} [25]
α^L	7×10^{-3} [25]
H_e	2500 Oe
h_x, h_y	$0.01 H_e$

proportional to the voltage generated by the ISHE, and is given by

$$I_L^\alpha(\boldsymbol{k}, \omega) = 2\alpha^L \, \mathrm{Im}[b_{\boldsymbol{k}}^*(x_1) \partial_t b_{\boldsymbol{k}}(x_1)]. \quad (10)$$

We are interested in the relative difference between the spin currents induced by the left- and right-moving spin waves in order to show a transverse spin transport, which we define as

$$\Delta(|\boldsymbol{k}|, \omega) = \frac{I_L^\alpha(\boldsymbol{k}, \omega) - I_L^\alpha(-\boldsymbol{k}, \omega)}{\max\left[\left|I_L^\alpha(\boldsymbol{k}, \omega)\right|, \left|I_L^\alpha(-\boldsymbol{k}, \omega)\right|\right]}. \quad (11)$$

Below, we consider this quantity in detail.

Results. The parameters used throughout this work are summarized in Table I. In Fig. 2 we show the difference between the spin current induced by left- and right-moving spin waves for different tilting angles of the magnetic field. For a magnetic field either completely in or out of plane there is no difference between the left and right lead (not shown). As we tilt the magnetic field out of plane a small difference becomes visible, which peaks at $\Delta = 1.25 \times 10^{-4}$ for $\phi_H = 60°$ and $2.5 < k < 12.5 \ \mu\mathrm{m}^{-1}$. As the tilting angle is further increased, the distribution of Δ shifts slightly, with the most notable change the movement of the maximum, which moves towards smaller wave vectors. We found that the relative difference Δ increases linearly with the bulk Gilbert damping constant. In order to measure this effect it might

therefore be beneficial to use a YIG thin film with deliberately introduced impurities such as rare-earth ions, to increase the damping [26], or even use a different ferromagnetic material with a higher Gilbert damping.

Numerically, we found that the relative difference Δ is nonzero even when the exchange coupling is artificially turned off, which indicates that only the dipole-dipole interaction is responsible for this effect. In the Supplemental Material [17] we show a full magnetostatic derivation of the eigenmodes for an obliquely magnetized thin film with only dipole-dipole interactions. Even though the energies are inversion symmetric, we find that the eigenmodes explicitly depend on

$$k_z \sin(2\phi_M), \quad (12)$$

which introduces an asymmetry between left- and right-moving spin waves if the magnetic field is tilted out of plane. A complete description of this problem also requires the inclusion of the exchange coupling, as was done in our numerical calculations. However, ignoring the exchange coupling allows us to demonstrate that the origin of the asymmetry between left- and right-moving spin waves lies in the the long-range dipole-dipole interaction carrying the inversion symmetry breaking of the interface.

Bozhko *et al.* [14] suggested a partial-wave picture to explain the transverse spin current. They reason that the profile along the film normal is made up by two partial waves, which have opposite momenta $\pm k_x$ and equal frequency ω if the film is magnetized in plane, thus canceling any transfer of angular momentum or energy. As the magnetic field is tilted out of plane, the two partial waves would, in this picture, no longer have opposite momenta, but still have the same frequencies. This would then allow for angular momentum transfer, but not energy transfer. With the magnetostatic calculation we are able to show that this picture is incomplete: The amplitudes of the two partial waves are asymmetric, not their momenta. This therefore allows both energy and angular momentum transfer, which we have confirmed numerically by evaluating $\langle \partial_t E \rangle$.

We found numerically that the region in k space where the relative difference Δ is significant has a lower bound related to the thickness of the thin film. Decreasing the thickness
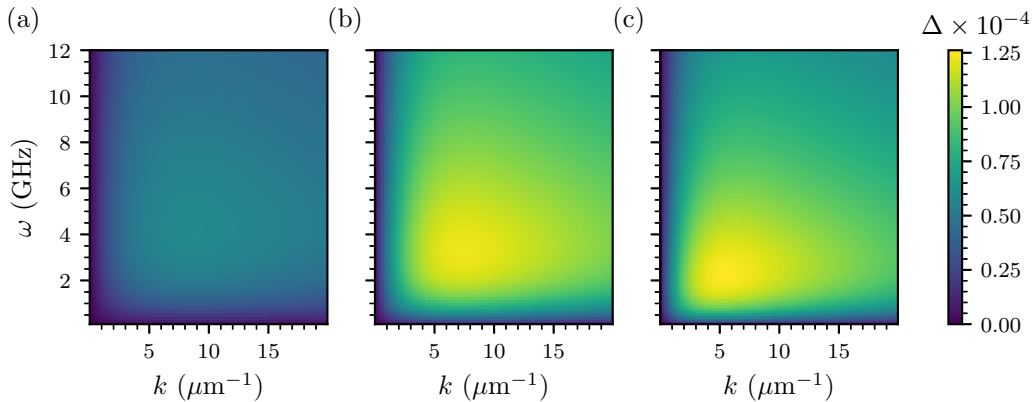

FIG. 2. The relative difference Δ between the spin current induced by left- and right-moving spin waves, as defined in Eq. (11), as a function of k and ω, for three different tilting angles of the magnetic field. The spin waves travel parallel to the in-plane projection of the magnetic field, such that $\boldsymbol{k} = k\hat{z}$. (a) $\phi_H = 30°$, $\phi_M = 18°$, (b) $\phi_H = 60°$, $\phi_M = 40°$, and (c) $\phi_H = 80°$, $\phi_M = 64°$. The peak difference is $\Delta(k = 7.5 \ \mu\mathrm{m}^{-1}, \omega = 4 \ \mathrm{GHz}) = 1.25 \times 10^{-4}$, when the field is tilted at an angle $\phi_H = 60°$. For a magnetic field completely in or out of plane (not shown) there is no discernible difference.

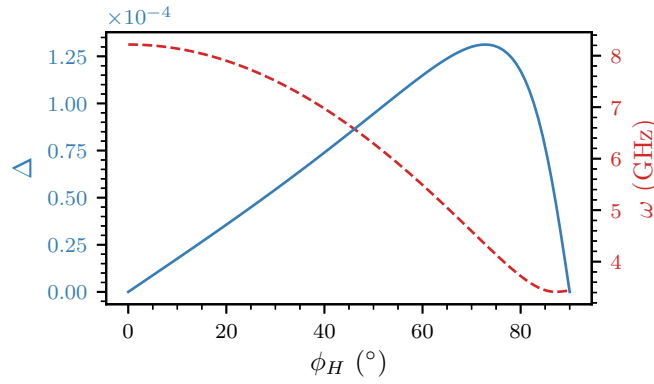FIG. 3. Relative difference between the spin current induced by left- and right-moving spin waves, Δ, as defined in Eq. (11), as a function of magnetic field tilt angle ϕ_H, for ω corresponding to the lowest mode in the spin-wave dispersion and fixed $k = 7.5 \ \mu\mathrm{m}^{-1}$ (solid line). Also shown is the frequency of the lowest mode as a function of the tilt angle (dashed line).

shifts the distribution as seen in Fig. 2 towards larger wave vectors. This can be traced to the fact that the long-wavelength magnetostatic magnon modes are standing waves [17], with wave vectors $\pm k_x$, where k_x is proportional to k_z. The standing waves need to have a wave vector big enough to fit at least one wavelength into the system, thus requiring that $k_z \gtrsim k_L$, where $k_L = 2\pi/d$. The reason for this coupling of the in-plane and out-of-plane directions is the long-range nature of the dipole-dipole interaction, ensuring that within our system the divergence of the magnetic field is zero, i.e., $\nabla \cdot \mathbf{B} = 0$. The maximum value of Δ does not change depending on the thickness of the film, only the location of the maximum. We have confirmed this numerically for the range $60 \leqslant d \leqslant 480$ nm. For even thinner films the maximum value of Δ becomes lower.

Excitation of magnons is only possible for values of ω determined by the spin-wave dispersion, with a minimum given by the lowest mode. We therefore show in Fig. 3 for fixed $k = 7.5 \ \mu\mathrm{m}^{-1}$ the evolution of the relative spin-current difference Δ as the magnetic field is tilted out of plane, with a driving at frequency ω corresponding to the lowest mode in the spin-wave dispersion. Also shown is the frequency of the lowest mode as a function of magnetic field tilt angle. It is clear that up to some critical value of the magnetic field angle Δ increases linearly, after which it falls off rapidly. It is also clear that the lowest mode is capable of transferring angular momentum along the film normal. This is contrary to the statements made by Bozhko *et al.* [14], who predicted that the lowest mode, which has a uniform profile, would not induce a transverse spin current. This is most likely due to the fact that in their work only the exchange current is considered, whereas we have taken all current contributions into account. Another possible explanation is their expansion in eigenfunctions of the second-order exchange operator, which might have failed to properly take the dipole-dipole interaction into account.

The different contributions to the transverse angular momentum transport, as defined in Eq. (9), are shown in Fig. 4 for left- and right-moving spin waves. We have set the bulk and interface damping to zero in order to clearly show the
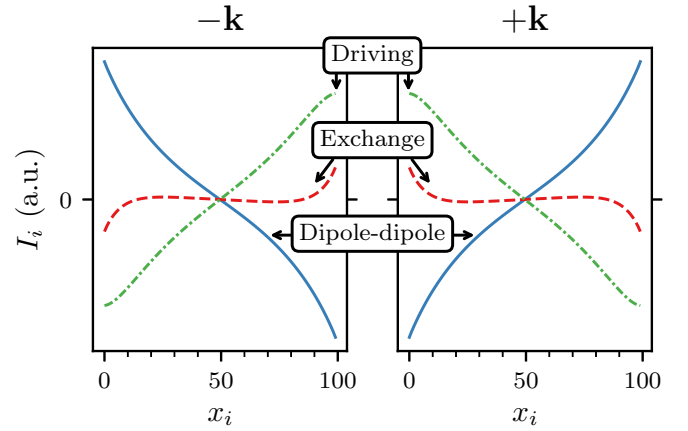

FIG. 4. The different contributions to the transfer of angular momentum along the film normal, where $I_i = \sum_j I_{i \to j}$ for the exchange and dipole-dipole interaction. The damping plays a negligible role in the transport of angular momentum, so it is turned off to illustrate the effects of the other contributions. The thickness of the thin film is reduced to $N = 100$ in order to better illustrate the variation through the film. The magnetic field is tilted out of plane with angle $\phi_M = 60°$ and the wave vector and driving frequency are fixed at $k = 30 \ \mu\mathrm{m}^{-1}$, $\omega = 4$ GHz.

exchange, dipole-dipole, and driving contributions to the transfer of spins along the film normal. First, we can see that there is a transport of angular momentum, even in the case of no spin absorption at the boundary, which agrees with the results by Bozhko *et al.* [14]. All contributions are zero in the case of an in-plane magnetic field (not shown)—if no spin sinks are attached. We can see that every contribution switches sign between left- and right-moving spin waves, as would be expected from symmetry. From this figure it is clear that the exchange spin current is not the only way the system transfers angular momentum. In fact, the contributions from the dipole-dipole interaction are larger than those of the exchange current. This shows that it is necessary to consider both interactions in order to gain a full understanding of the transport of angular momentum in the transverse direction. Also note that since the dipole-dipole contribution is nonzero, there is a finite torque on the system, which could be measured in a cantilever experiment [27].

Conclusion and discussion. In this Rapid Communication we have shown, using microscopic linear spin-wave theory, that there is a flow of angular momentum, or spin current, along the film normal in obliquely magnetized thin films. This can be measured using an antenna-detector setup, where the spin current induced by the left- and right-moving spin waves will be different, proving the existence of a transverse spin current. This effect can be used as a way to manipulate the spin current flowing along the film normal, for example, by controlling the magnetic field angle. We have also demonstrated that this spin current is the result of the dipole-dipole interactions in the film, which carry the inversion breaking at the interface.

We have not considered explicitly the interactions of the spin waves with the lattice. The dipole-dipole interactions couple the magnons to the lattice and therefore angular momentum can be transferred from and to the phonons,

which can also transport angular momentum [28–30]. A more complete description of the system should therefore include these phonon-magnon interactions, but this is beyond the scope of this Rapid Communication.

[1] L. J. Cornelissen, J. Liu, R. A. Duine, J. B. Youssef, and B. J. van Wees, Long-distance transport of magnon spin information in a magnetic insulator at room temperature, Nat. Phys. **11**, 1022 (2015).

[2] B. L. Giles, Z. Yang, J. S. Jamison, and R. C. Myers, Long-range pure magnon spin diffusion observed in a nonlocal spin-Seebeck geometry, Phys. Rev. B **92**, 224415 (2015).

[3] R. L. Stamps, S. Breitkreutz, J. L. Akerman, A. V. Chumak, Y. Otani, G. E. W. Bauer, J.-U. Thiele, M. Bowen, S. A. Majetich, M. Kläui, I. L. Prejbeanu, B. Dieny, N. M. Dempsey, and B. Hillebrands, The 2014 magnetism roadmap, J. Phys. D: Appl. Phys. **47**, 333001 (2014).

[4] G. Csaba, Á. Papp, and W. Porod, Perspectives of using spin waves for computing and signal processing, Phys. Lett. A **381**, 1471 (2017).

[5] S. Klingler, P. Pirro, T. Brächer, B. Leven, B. Hillebrands, and A. V. Chumak, Spin-wave logic devices based on isotropic forward volume magnetostatic waves, Appl. Phys. Lett. **106**, 212406 (2015).

[6] A. Khitun, M. Bao, and K. L. Wang, Magnonic logic circuits, J. Phys. D: Appl. Phys. **43**, 264005 (2010).

[7] A. Khitun and K. L. Wang, Non-volatile magnonic logic circuits engineering, J. Appl. Phys. **110**, 034306 (2011).

[8] A. V. Chumak, A. A. Serga, and B. Hillebrands, Magnon transistor for all-magnon data processing, Nat. Commun. **5**, 4700 (2014).

[9] T. Schneider, A. A. Serga, B. Leven, B. Hillebrands, R. L. Stamps, and M. P. Kostylev, Realization of spin-wave logic gates, Appl. Phys. Lett. **92**, 022505 (2008).

[10] T. Fischer, M. Kewenig, D. A. Bozhko, A. A. Serga, I. I. Syvorotka, F. Ciubotaru, C. Adelmann, B. Hillebrands, and A. V. Chumak, Experimental prototype of a spin-wave majority gate, Appl. Phys. Lett. **110**, 152401 (2017).

[11] G. A. Melkov, A. A. Serga, V. S. Tiberkevich, A. N. Oliynyk, and A. N. Slavin, Wave Front Reversal of a Dipolar Spin Wave Pulse in a Nonstationary Three-Wave Parametric Interaction, Phys. Rev. Lett. **84**, 3438 (2000).

[12] A. V. Sadovnikov, S. A. Odintsov, E. N. Beginin, S. E. Sheshukova, Y. P. Sharaevskii, and S. A. Nikitov, Toward nonlinear magnonics: Intensity-dependent spin-wave switching in insulating side-coupled magnetic stripes, Phys. Rev. B **96**, 144428 (2017).

[13] A. V. Chumak, V. I. Vasyuchka, A. A. Serga, and B. Hillebrands, Magnon spintronics, Nat. Phys. **11**, 453 (2015).

[14] D. A. Bozhko, H. Y. Musiienko-Shmarova, V. S. Tiberkevich, A. N. Slavin, I. I. Syvorotka, B. Hillebrands, and A. A. Serga, Unconventional spin currents in magnetic films, Phys. Rev. Research **2**, 023324 (2020).

[15] E. Saitoh, M. Ueda, H. Miyajima, and G. Tatara, Conversion of spin current into charge current at room temperature: Inverse spin-Hall effect, Appl. Phys. Lett. **88**, 182509 (2006).

[16] Y. Tserkovnyak, A. Brataas, and G. E. W. Bauer, Enhanced Gilbert Damping in Thin Ferromagnetic Films, Phys. Rev. Lett. **88**, 117601 (2002).

[17] See Supplemental Material at http://link.aps.org/supplemental/10.1103/PhysRevB.101.220407 for the full form of the amplitude factors in Eq. (8), the dispersions, the details of the magnetostatic calculation, and the explicit form of the terms in the continuity equation for the spin in Eq. (9).

[18] L. Fallarino, M. Madami, G. Duerr, D. Grundler, G. Gubbiotti, S. Tacchi, and G. Carlotti, Propagation of spin waves excited in a permalloy film by a finite-ground coplanar waveguide: A combined phase-sensitive micro-focused Brillouin light scattering and micromagnetic study, IEEE Trans. Magn. **49**, 1033 (2013).

[19] A. V. Chumak, A. A. Serga, M. B. Jungfleisch, R. Neb, D. A. Bozhko, V. S. Tiberkevich, and B. Hillebrands, Direct detection of magnon spin transport by the inverse spin Hall effect, Appl. Phys. Lett. **100**, 082405 (2012).

[20] V. Cherepanov, I. Kolokolov, and V. L'vov, The saga of YIG: Spectra, thermodynamics, interaction and relaxation of magnons in a complex magnet, Phys. Rep. **229**, 81 (1993).

[21] J. Zheng, S. Bender, J. Armaitis, R. E. Troncoso, and R. A. Duine, Green's function formalism for spin transport in metal-insulator-metal heterostructures, Phys. Rev. B **96**, 174422 (2017).

[22] S. Geller and M. A. Gilleo, The crystal structure and ferrimagnetism of yttrium-iron garnet, $Y_3Fe_2(FeO_4)_3$, J. Phys. Chem. Solids **3**, 30 (1957).

[23] B. R. Tittmann, Possible identification of magnetostatic surface spin wave modes in ferromagnetic resonance on epitaxial yttrium-iron-garnet films, Solid State Commun. **13**, 463 (1973).

[24] A. Kreisel, F. Sauli, L. Bartosch, and P. Kopietz, Microscopic spin-wave theory for yttrium-iron garnet films, Eur. Phys. J. B **71**, 59 (2009).

[25] M. Haertinger, C. H. Back, J. Lotze, M. Weiler, S. Geprägs, H. Huebl, S. T. B. Goennenwein, and G. Woltersdorf, Spin pumping in YIG/Pt bilayers as a function of layer thickness, Phys. Rev. B **92**, 054437 (2015).

[26] V. Sharma and B. K. Kuanr, Magnetic and crystallographic properties of rare-earth substituted yttrium-iron garnet, J. Alloys Compd. **748**, 591 (2018).

[27] K. Harii, Y.-J. Seo, Y. Tsutsumi, H. Chudo, K. Oyanagi, M. Matsuo, Y. Shiomi, T. Ono, S. Maekawa, and E. Saitoh,

Spin Seebeck mechanical force, Nat. Commun. **10**, 2616 (2019).

[28] S. Vonsovskii and M. Svirskii, Phonon spin, Sov. Phys. Solid State **3**, 1568 (1962).

[29] A. T. Levine, A note concerning the spin of the phonon, Nuovo Cimento **26**, 190 (1962).

[30] L. Zhang and Q. Niu, Angular Momentum of Phonons and the Einstein–de Haas Effect, Phys. Rev. Lett. **112**, 085503 (2014).